ELSEVIER

Spectrochimica Acta Part B 62 (2007) 1208 – 1215

SPECTROCHIMICA ACTA PART B

www.elsevier.com/locate/sab

Spectroscopic characterization of a microplasma used as ionization source for ion mobility spectrometry

Antje Michels [a], Sven Tombrink [a], Wolfgang Vautz [a], Manuela Miclea [b], Joachim Franzke [a,*]

[a] *ISAS—Institute for Analytical Sciences, Dortmund and Berlin, Bunsen-Kirchhoff-Strasse 11, D-44139 Dortmund, Germany*
[b] *Martin Luther University Halle-Wittenberg, Physics Faculty, Dept. of Optics, Hoher Weg 8, D-06120 Halle (Saale), Germany*

Received 14 March 2007; accepted 10 August 2007
Available online 19 August 2007

Abstract

We report a miniaturized excitation source for soft ionization of molecules based on a dielectric barrier discharge. An atmospheric plasma is established at the end of a 500 μm diameter capillary using He as buffer gas. The plasma jet which comes out of the capillary is dependent on the gas flow rate. The mechanism of the production of N_2^+ outside the capillary, which is relevant for the protonation of molecules and sustains the production of primary ions, is investigated by spatially resolved spectroscopic measurements throughout the plasma. Possible application of such miniaturized plasmas is the ionization of gaseous compounds under atmospheric pressure as an alternative to traditional APCI (atmospheric pressure chemical ionization). The miniaturized plasma was applied as ionization source for ion mobility spectrometry where the common sources are radioactive, thus limiting the place of installation. First measurements of gaseous compounds with such a plasma ion mobility spectrometer with promising results showed detection limits comparable or even better than those obtained using common radioactive ionization sources.

Keywords: Dielectric barrier discharge; Miniaturized atmospheric plasma; Ion mobility spectrometry

1. Introduction

Microplasmas operated either at atmospheric or reduced pressure exist in various configurations. Among these there are direct current (dc) glow discharges used as molecular emission detectors (e.g., [1–4]), electrolyte-as-cathode glow discharges (ELCAD, e.g. [5–9], liquid-sampling atmospheric pressure glow discharges (LS-APGD, e.g. [10–13]), miniature inductively coupled plasmas (e.g. [14–16]), capacitively coupled radio-frequency (cc-rf) discharges (e.g. [17–22]), microwave induced plasmas based on the microstrip technology (e.g., [23–25]), microstructured electrode discharges (MSD, e.g. [26,27]), dielectric barrier discharges (DBDs, e.g. [28–32]), and some other variations (e.g., [33]). Several review papers can be found in the literature, giving an overview and a description of these different types of analytical microplasmas [34–37]. Moreover, microplasmas in various configurations are also of great interest for applications other than analytical spectrometry [38].

A DBD is typically formed between two parallel electrodes, with a gap distance in the order of 0.1–10 mm. One or both electrodes are covered with a dielectric barrier. Hence, the DBD cannot be operated with direct current (dc), because of dielectric charging issues. Typically, they are operated with square wave currents, sinusoidal wave currents, or pulsed waveforms with a frequency ranging from a few Hz to MHz, and mostly in the kHz-range [39]. The dielectric constant and thickness of the dielectric determine the amount of displacement current that can flow through the dielectric. DBDs often operate at atmospheric pressure but they are strongly non-equilibrium plasmas. They possess unique features and characteristics which have provided the basis for a host of applications like ozone generation, gas treatment, excimer lamps, plasma display panels and surface-engineering including cleaning, activation and coating deposition [40–48].

The characteristics of a DBD plasma, developed to be used in atomic absorption spectrometry, are described in [28–31]. These DBDs were demonstrated to be small, low electric power (<1 W), low gas temperature (~600 K) plasma sources, with excellent dissociation capability for molecular species and have

* Corresponding author. Tel.: +49 231 1392 174; fax: +49 231 1392 120.
E-mail address: franzke@isas.de (J. Franzke).

0584-8547/$ - see front matter © 2007 Elsevier B.V. All rights reserved.
doi:10.1016/j.sab.2007.08.004

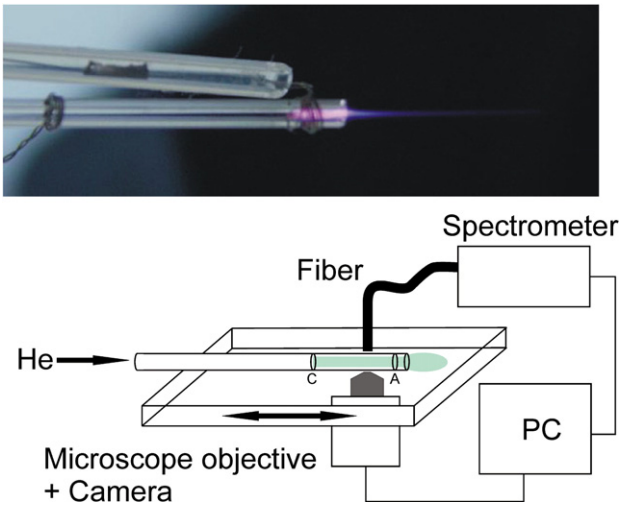

Fig. 1. Photograph of the plasma source and the experimental arrangement.

been used in plasma modulation diode laser atomic absorption spectrometry of excited states of chlorine and fluorine, with typically helium or argon as the plasma gases. These discharges operated at reduced pressures (10–100 mbar). A further decrease of the discharge dimensions and a higher supply voltage enables the maintenance of the discharge at atmospheric pressure.

In the present report the plasma is operated in a capillary surrounded by two ring electrodes, an arrangement comparable to that used by Guchardi and Hauser [49] or Laoussi and Lu [50]. The dielectric barrier discharge is at the end of the capillary and the gas flow will extend the plasma out of the capillary.

It is known that the detection limit of atomic absorption or emission spectrometry of elements with metastable levels decreases drastically when air (particularly nitrogen) is involved. However, the present work will focus on the study of the characteristics of this DBD used as soft ionization source of molecules. Furthermore, experiments by coupling the DBD with ion mobility spectrometry will be discussed to illustrate the potential use of the miniaturized plasma as an alternative to APCI. Ion mobility spectrometry is a rapid and sensitive method for the detection of gas phase compounds [51]. The method was first applied for the detection of chemical warfare analytes, drugs and explosives. In recent years the ion mobility spectrometry is increasingly in demand for process control, food quality and safety [52,53] and for medical applications [54,55]. The spectroscopic characterization of the microplasma will therefore be of essential relevance in view of the foreseen application of such plasmas.

1.1. Atmospheric Pressure Chemical Ionization (APCI)

Chemical ionization at atmospheric pressure (APCI) has its primary applications in the area of ionization of gas phase compounds — usually evaporated samples from liquid chromatography [56,57]. The corona discharge replaces the electron beam in chemical ionization and produces primary N_2^+ and N_4^+ ions by electron ionization impact [58]. Another possible ionization source is β radiation which is used most commonly in ion mobility spectrometry [51].

The formation of the so-called reactant ions N_2^+ generate protonated water clusters which in turn protonates analyte molecules [59,60]. Once the ions are formed, they enter the pumping and focussing stage of a mass spectrometer or they are moved by an electric field towards the drift region of an ion mobility spectrometer.

Besides corona discharges, the most common source in ion mobility spectrometer [51] (IMS) is a radioactive ^{63}Ni foil, analogous to those applied in electron capture detectors. ^{63}Ni emits β particles with a continuous energy distribution. The β particles lose energy during collisions with the drift gas; the average energy loss per ion pair formed in N_2 is 35 eV, with ionization only occurring as long as the energy of the β particles remains above the ionization potential of N_2, 15.58 eV [61]. The process starts with the formation of electrons which then initiate the generation of N_2^+ primary ions and lead to the same reactions as described above.

2. Experimental

2.1. Dielectric barrier discharge

Fig. 1 shows a photograph of the dielectric barrier discharge with a plasma cone outside the electrode region and a schematic experimental arrangement. In the following, this plasma cone will be called plasma jet. The discharge consists of a 3 cm long glass capillary with an inner diameter of 500 μm and an outer diameter of 1.2 mm. Silver cables of 500 μm diameter are wrapped around the capillary forming electrodes with a separation distance of 12 mm. The distance of the electrode to the end of the capillary is 2 mm. One electrode cable is isolated in order to prevent any discharge outside the capillary. He 5.0, which has a purity of 99.999% and an impurity of 3 ppm N_2, is used as plasma gas at atmospheric pressure. Three different flow rates of He (70 mL/min, 350 mL/min and 750 mL/min) are established in the capillary. Unlike the DBDs used for diode laser atomic absorption spectrometry, where the terminals of the power supply were ground-free (the electrode voltage is changed between positive and negative voltage), here a periodic positive voltage pulse (5.5 kV with a frequency of 33 kHz and a pulse width of 2 μs) is applied. The discharge is initiated between the electrodes to form a plasma outside the capillary and dependent on the gas flow.

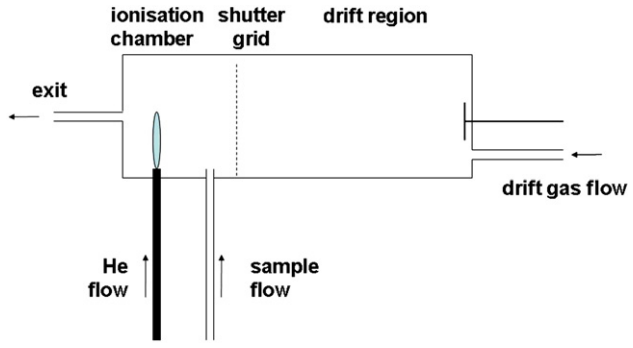

Fig. 2. Scheme of the experimental arrangement of the ion mobility spectrometer with the miniaturized plasma as ionization source.

Table 1
Experimental parameters of the ion mobility spectrometer designed at ISAS using a miniaturized plasma as ionization source

IMS	Drift tube	12 cm, 1.5 cm diameter
	Electric field	330 V/cm
	Grid opening time	300 μs
	Drift gas	N_2
	Drift gas flow	100 mL/min
	Sample gas	N_2
	Sample gas flow	150 mL/min
Plasma	Voltage	5.5 kV
	Frequency	33 kHz
	Capillary diameter, distance of electrodes	500 μm, 12 mm
	He purity	99.999%
	He flow	250 mL/min

The schematic experimental arrangement shows the discharge capillary connected onto a movable stage of a microscope in order to photograph the plasma light at certain positions (Sony CCD color video camera XC-999/999P). Optical emission spectra (integration time 10 ms) were taken with an Ocean Optics spectrometer (USB2000) as a function of the position using a glass fiber (Ocean Optics QP200-2-VIS-BX, 200 μm) adjusted perpendicular to the capillary.

2.2. Ion mobility spectrometry

Although the principles are well known a brief discussion pertinent to the present work is given here. Analyte molecules are ionized by charge transfer of the reactant ions, protonated water clusters derived from a reaction as described in Section 1.1. The ions are moved in an electric field towards the detector, a Faraday plate. During their drift they collide with the drift gas molecules moving in the opposite direction, thus being decelerated. The collision frequency depends on their mass, charge and shape and therefore their drift time as a measure for their mobility which is characteristic for the ion. The ion current relates to the concentration of the analyte in the ionization region. The drift time of the ions in the present drift gas can be corrected to the pressure and the temperature of the drift gas, thus obtaining the so-called reduced ion mobility

$$K_0 = (L/Et)\cdot(p/p_0)\cdot(T_0/T) \quad (1)$$

with K_0 reduced ion mobility (ion mobility $K=L/(E\cdot t)$), L length of the drift distance (cm), E electric field strength (V/cm), t drift time (s), p pressure of the drift gas in (hPa), p_0 atmospheric pressure: $p_0=1013.2$ hPa, T temperature of the drift gas (K) and $T_0=273.2$ K.

Radioactive ionization sources (e.g. ^{63}Ni) are commonly used. There radiation ionizes the available drift gas and the so-called reactant ions (protonated water clusters like $(H_20)_nH^+$, [51]) can be detected with the IMS. When an analyte is introduced into the ionization region, the reactant ions transfer their charge to the analyte molecules resulting in a decrease of the reactant ion peak (RIP) and an increase of an analyte peak.

The miniaturized plasma was applied to an ion mobility spectrometer (IMS) which was designed at ISAS — Institute for Analytical Sciences and applied for food quality and safety and breath analysis. The detailed instrumentation is described elsewhere [52–55]. The plasma was implemented in the IMS orthogonal to the gas flow as shown in Fig. 2 — this arrangement obtained higher yield of ions than the implementation axial to the gas flow for the same instrumentation. The instrument was operated under ambient pressure and temperature with the experimental parameters as listed in Table 1.

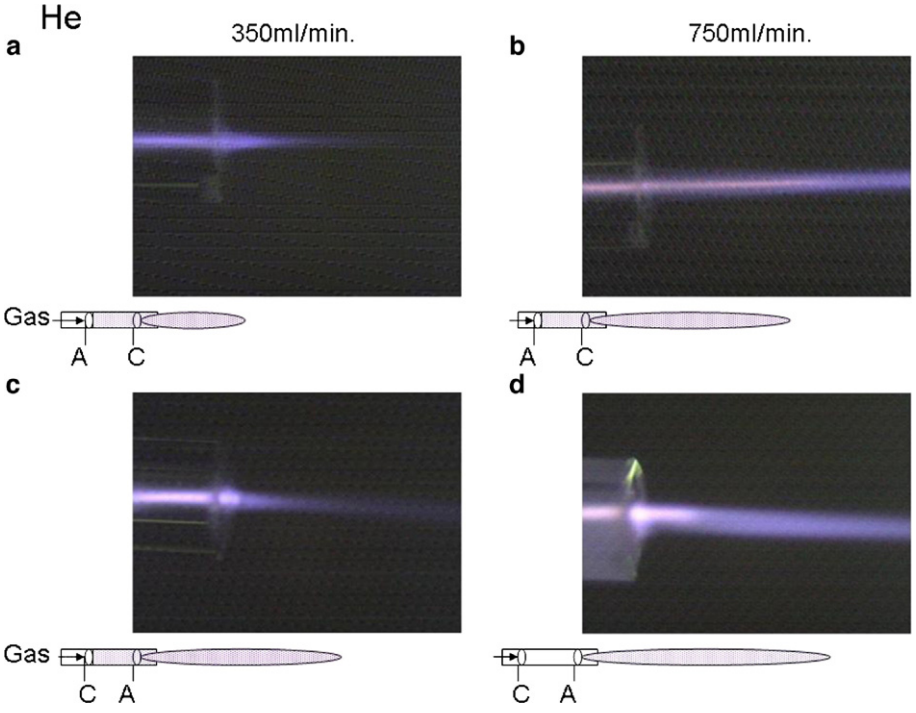

Fig. 3. Plasma at the end of the capillary with different flow rates (350 mL/min, 750 mL/min) and different electrode polarities.

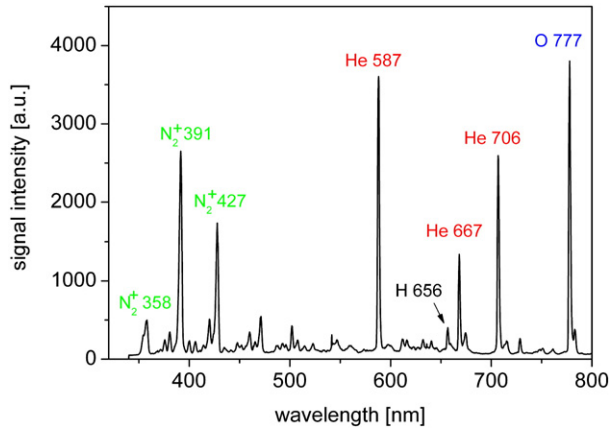

Fig. 4. Experimental emission spectrum obtained in the vicinity of the electrode.

Detection limits of IMS in general are determined by exponential dilution of a suitable starting concentration (usually in the range of few hundred ppb).

3. Results and discussion

To investigate the geometrical extension of the plasma jet, different polarities and flow rates were tested. Photographs of jets and the corresponding different polarities of the electrodes and the flow rates are shown in Fig. 3. The arrangements shown refer to the cathode in the vicinity of the capillary outlet (Fig. 3a and b) and the anode close to the end of the capillary (Fig. 3c and 3d). In Fig. 3a and 3c a flow of 350 mL/min was used and in Fig. 3b and 3d the flow was 750 mL/min.

In all cases the plasma propagates outside the capillary as a plasma jet. When He is used as plasma gas, for both flow rates the plasma length outside the discharge is longer when the anode is at the outlet side. Since the discharge is evaluated as an APCI source for molecules at atmospheric pressure outside the plasma-capillary this is the configuration of choice. The length

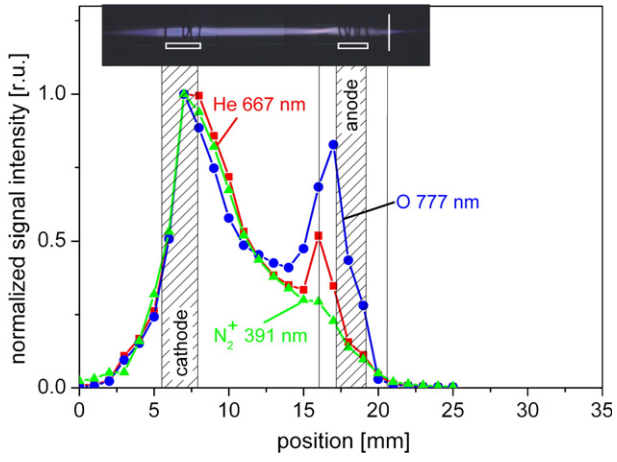

Fig. 5. Normalized intensities of the O 777 nm, He 667 nm and N_2^+ emission lines as a function of measurement position. The gas flow was 70 mL/min. A photograph using a CCD color video camera shows the length of the electrodes marked by a rectangle and the outlet of the capillary by a line. The photograph illustrates the positions of measurement.

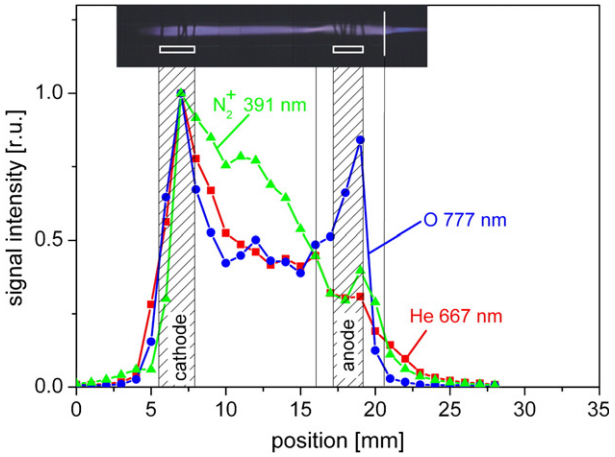

Fig. 6. Spatial distribution of O 777 nm, He 667 nm and N_2^+ emission lines. The gas flow was 350 mL/min.

and the brightness of the plasma jet increase with higher flow rates. Optical emission spectra are taken along the plasma propagation length to investigate processes occurring inside the plasma, in and outside the capillary.

One of these spectra, representative for the emission region between the electrodes close to the cathode is shown in Fig. 4. The flow was 70 mL/min and the most intense lines were different molecular ion lines of N_2^+ 358, 391, 427 nm [62] originated from the impurity in He 5.0, atomic lines of He 587, 667, 706 nm, and the O 777 nm line [63]. The intensities of all these lines drastically depend on the flow rate and the position of observation. Spectra are taken at different positions of the plasma between the electrodes and behind the anode outside the capillary. Since the electrodes are made by 100 μm diameter platinum wires, which are wrapped around the capillary, the emission could be measured through the spaces in between the wires.

The results are shown in Figs. 5–7. Three different He flow rates of 70 mL/min (Fig. 5), 350 mL/min (Fig. 6) and 750 mL/min (Fig. 7) were used and the spatial dependence of two atomic lines (He 667 nm line and O 777 nm line) and one molecular

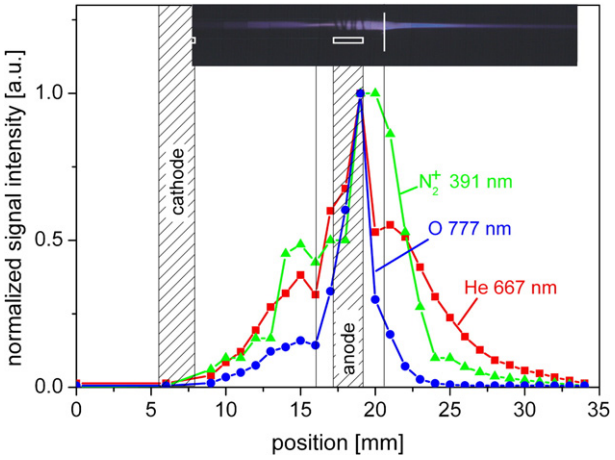

Fig. 7. Spatial distribution of O 777 nm, He 667 nm and N_2^+ emission lines. The gas flow was 750 mL/min.

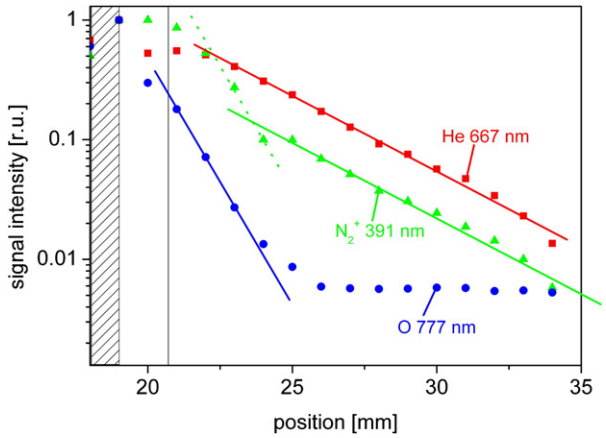

Fig. 8. Spatial distribution of O 777 nm, He 667 nm and N_2^+ emission line intensities behind the anode. The gas flow was 750 mL/min.

line N_2^+ 391 nm was measured. In order to investigate the influence of He on N_2^+ a normalized representation of the intensities along the axis of the plasma is chosen for Figs. 5, 6 and 7. Each graph is supported with a photograph to relate the spectra with the position of the measurements. Both areas where the electrodes are placed are marked with a white rectangle. The cathode is on the left, the anode on the right side and the capillary outlet is marked with a white line.

The spatial dependence of the emission of He excited and O-metastable states as well as the N_2^+ 391 nm shows two maxima in Fig. 5, where a flow rate of 70 mL/min was used. The left maximum is located at the position of the cathode and the other is in front of the anode.

A similar behavior is shown in DBDs applied for diode laser atomic absorption spectrometry, where the distance between the temporary cathode and the absorption maximum is pressure-dependent [29–33], i.e., approximately 400 and 200 μm for 10 and 50 mbar, respectively. This behaviour is similar to that occurring in a glow discharge, where the negative glow is shifted towards the cathode if the pressure increases. In this case the terminals of the power supply were ground-free (one electrode is negative while the other electrode is positive and vice versa). As consequence, the location of the absorption maximum switched from the vicinity of one electrode to the other, like in a glow discharge with changing polarities. In the present case, a periodic pulsed voltage with a positive polarity was applied. Therefore, like the above cited discharge, the present discharge resembles a glow discharge periodically starting from the cathode side. Despite the dominant opinion that DBDs are Townsend discharges [64] and normally involve streamer breakdown as for corona discharges, the question of the origin of the breakdown is still open especially for the very beginning of the discharge [65]. The discharge described here has similarities to a glow discharge, with the left maximum correlating with the negative glow. The cathode fall length, d_c, covers the distance from the cathode surface up to the cathodic limit of the negative glow.

It has to be underlined that the cathode zones are critical for sustaining the discharge because the ionization and excitation takes place mostly in this region. If the distance between the electrodes is smaller than the length of the cathode fall, the discharge extinguishes because the electrons do not gain enough energy to produce ionization even if the electric field is high [66]. As an example, for He the normal cathode fall should be between 60 and 180 V, while the pd (pressure-dimension) product [67] of the pressure and cathode fall thickness is about 1.3 Torr cm. Using this value, at 10 mbar the cathode fall thickness should be about 1.7 mm, at 100 mbar about 170 μm and at 1 bar about 17 μm.

The electrodes consist of wires with several coils wrapped around the capillary and have a spatial elongation of about 2 mm. Since the discharge is maintained under atmospheric pressure, the distance between the cathode and the negative glow is in the micrometer range. Therefore, and due to the fact that the electrodes are comparable with hollow cathodes, the maximum emission intensity is located between the inner diameter and the center of the capillary in the radial direction inside the cathode. The distances calculated above (17 μm) and also observed (at the position of the cathode) are comparable with the conditions to be expected in dielectric barrier discharges. A difference between a glow discharge and a dielectric barrier discharge might be the production of electrons. In the case of a glow discharge the secondary electrons are emitted from the cathode metal surface. In the case of the dielectric barrier discharge the secondary emission coefficient of glass is smaller than that of a metal surface so that the electrons cannot be emitted only from the glass surface of the dielectric layer but they can be produced by ion-neutral collisions near the dielectric surface.

It is obvious from the photos as well as from the intensities measured in and outside the electrodes that the emission maximum shown in Fig. 5 is shifted towards the anode (Fig. 6) and out of the region in between the electrodes (Fig. 7). In discharge tubes with diameters in the range of 5–20 mm this effect could not be observed. When the flow is about 750 mL/min and the diameter of the capillary is 500 μm, the velocity of an atom is about 60 m/s. Generally, the first maximum indicates the position of the negative glow. When the negative glow is transported away from the cathode, the electric field between the cathode and the negative glow (a positive space charge) would diminish drastically and the discharge should extinguish. But the discharge is not extinguished even when the negative glow has a distance from the cathode of a few mm (usually expected to be in the micrometer range). Therefore, the whole system, which is determined by the position where the electrons are created and the negative glow, will be shifted in the direction of the anode and beyond. Since a discharge will not be extinguished when the positive column is eliminated the shifted system will support the discharge as long as the negative glow will not extend the position of the anode. This supports the assumption that the electrons are produced by ion-neutral collisions. In order to ionize buffer gas atoms and therefore to produce electrons the velocity of ions calculated by the kinetic energy of an He^+ ion, which is sufficient to ionize a He atom (24.56 eV) needs to be nearly 3 orders of magnitude higher than the velocity initiated by the flow of 750 mL/min (60 m/s). With a Paschen-voltage of about 240 V and a “cathode fall thickness” of about 20 μm, which is the gap between the position where

electrons are produced and the start of the negative glow, the velocity

$$\vec{u} = (e\lambda/2m\bar{v})\vec{E} \quad (2)$$

(λ mean free path, m mass, $\bar{v}$ mean velocity, E electric field) of the He^+-ions is sufficiently high to produce electrons [68].

When the ring anode with its radius R is regarded as a line charge a field distribution along the electrode ring-axis of the capillary

$$E_x = Qx/4\pi\varepsilon_0(R^2 + x^2)^{3/2} \quad (3)$$

is induced beyond both sides of the anode (E_x electric field along the axis, Q charge, R radius of the electrode ring, x position along the axis). Beyond the anode in the direction of the outlet the field increases, reaches its maximum at a distance L of $R/(2^{1/2})=0.9$ mm and decreases for $L \gg R$ like the field of a point charge $E_x=Q/4\pi\varepsilon_0 x^2$. Due to this field distribution, ions react differently than neutral species and atoms in excited states. In any case, all excited and ionized atoms and molecules will be de-excitated by collisions outside the discharge region between the electrodes. As can be seen from Fig. 7, N_2^+ reaches more out of the capillary than excited O due to the fact that N_2^+ will be accelerated in the field behind the electrode. Therefore, N_2^+ de-excitation to N_2 might be shifted in the direction of the outlet compared with the de-excitation of excited O* or He* atoms (position: 20 mm). In case of He, which is the buffer gas, the measurement identifies not only excited He* atoms but also He^+ ions, which are accelerated as well a N_2^+ ions by the electric field. Due to the lower mass of He^+, the de-excitation to excited He* states and the following de-excitation to metastable low level excited atoms may take place at a position even more shifted than the position where the de-excitation of N_2^+ occurs (position: 21 mm). It can be seen that the slope of the He^+ recombination is less steep than that of O^+ and N_2^+. Moving away 2 mm further the slope of N_2^+ recombination is changed. This might be due to the fact that N_2 molecules will be excited or re-excited by He excited atoms. This can be clearly seen in Fig. 8, which reproduces a part of Fig. 7 with the signal intensity in a logarithmic scale. This graph shows a change of the slope at the 24 mm position. The slope of N_2^+ for positions lower than 25 mm is parallel to the slope of O* and the slope for positions higher than 25 mm has the same slope as the slope of He*. This supports the assumption that the N_2^+ recombination is definitely influenced by excited He* atoms line outside the electrodes and the capillary.

He^+, He* and N_2^+ extend from the capillary and will be directly or indirectly responsible for the production of protonated analyte ions as described above with the reactions proceeding in the corona discharge region during APCI or reactions initiated by a radioactive ^{63}Ni foil in IMS.

3.1. Application of the microplasma to IMS: a selected example

As an example of application, the microplasma was used as ionization source in an ion mobility spectrometer (IMS), and the results of first experiments are given in Fig. 9a. The light gray line represents the spectra of the IMS with the microplasma ionization source described before. The first peak with the ion mobility $K_o=2.06$ cm^2/Vs (RIP) is caused by the reactant ions — protons clustered with water molecules $(H_2O)_n H^+$, which are formed by ionization of the drift gas. The solid line represents the ion mobility spectrum from a sample of 55 ppb 2-heptanone as a reference analyte. The minor peaks in the spectra are caused by contamination of the instrument. When 2-heptanone at a concentration of 55 ppb is introduced (solid line), the reactant ions transfer their charge to the analyte molecules, thus leading to a decrease of the RIP and the formation of two analyte ion peaks.

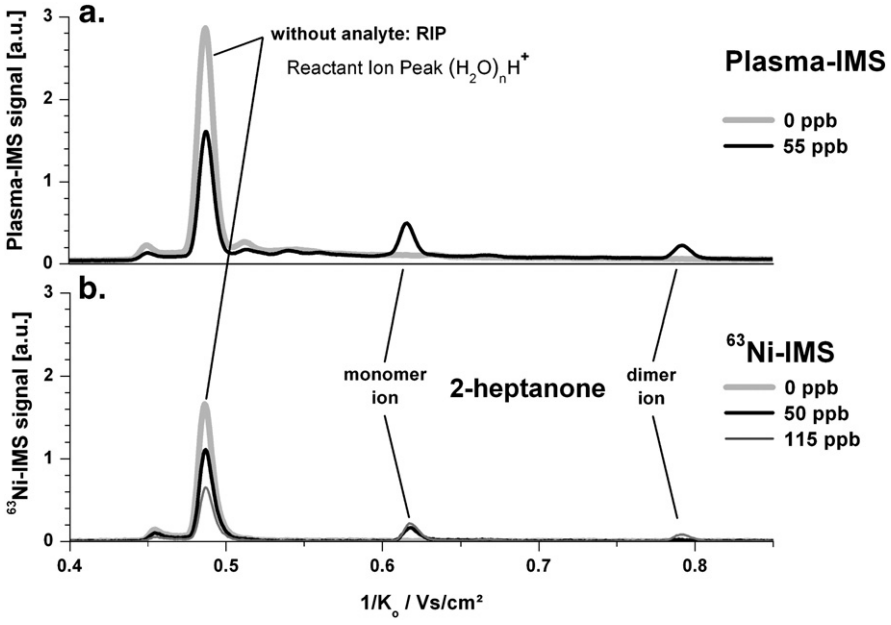

Fig. 9. Ion mobility spectra with 2-heptanone in lower ppb concentrations and without the analyte detected with the plasma-IMS (a) and a ^{63}Ni-IMS (b).

The peak at 1.61 cm^2/Vs represents the protonated monomer (MH^+) and the second one at 1.25 cm^2/Vs the protonated dimer ($2MH^+$). Dimer ions are formed, when a particular ion concentration – which depends on the analyte – in the ionization region of the IMS is exceeded. Therefore, the occurrence of dimer ions is not only a measure for the analyte concentration but also for the ionization yield. Fig. 9b shows the corresponding spectra of the RIP (light gray) and two concentrations of 2-heptanone (50 ppb — black solid line and 115 ppb — gray solid line). The dimer ion is formed only when the 115 ppb sample concentration is introduced — for 50 ppb only the monomer ion is left. All experiments were repeated 5 times with good reproducibility. The relative standard deviation of the RIP peak height was less than 2% for the ^{63}Ni-IMS and less than 4% for the Plasma-IMS.

The IMS signal is 1.3 times higher from the plasma IMS compared to the ^{63}Ni-IMS. Considering that the same amplifier and electronics were used for the operation of both IMS, this can only be explained by a higher ionization yield of the plasma ionization source. Consequently, for a concentration of 55 pbb, dimer ions are still formed in the Plasma-IMS but no longer in the ^{63}Ni-IMS for a similar concentration (50 ppb). Therefore the plasma IMS seems to be more sensitive, which corresponds to the detection limits which were found in the range of 20 ppb for the ^{63}Ni-IMS and in the range of 5 ppb for the Plasma-IMS.

4. Conclusions

A dielectric barrier discharge produced in a capillary by applying positive pulses from an ac generator was presented and its spectroscopic behavior discussed, as a soft ionization source for analyte molecules in air. Optical emission spectra of the discharge inside and outside the capillary appear to show a behavior similar to that observed with a normal glow discharge modified by the presence of strong electric fields in the vicinity of the cathode and by the relatively high gas flow through the capillary. It is argued here that the excited noble gas atoms and the nitrogen ions are responsible for the soft ionization of the analyte. The prospective for replacing the Ni β emitting source or the corona discharge in ion mobility spectrometers is very promising. Further optimization and a detailed comparison of the detection limits and the selectivity of both ^{63}Ni-IMS and Plasma-IMS as well as mass spectroscopy investigations of the ions formed by the miniaturized plasma will be carried out in the near future.

Acknowledgements

The financial support by the *Ministerium für Innovation, Wissenschaft, Forschung und Technologie des Landes Nordrhein-Westfalen*, by the *Bundesministerium für Bildung und Forschung*, and by the *Deutsche Forschungsgemeinschaft (DFG)* is gratefully acknowledged.

References

[1] J.C.T. Eijkel, H. Stoeri, A. Manz, An atmospheric pressure dc glow discharge on a microchip and 1st application as a molecular emission detector, J. Anal. At. Spectrom. 15 (2000) 297–300.
[2] J.C.T. Eijkel, H. Stoeri, A. Manz, A dc microplasma on a chip employed as an optical emission detector for gas chromatography, Anal. Chem. 72 (2000) 2547–2552.
[3] H.J. Kim, Y.A. Woo, J.S. Kang, S.S. Anderson, E.H. Piepmeier, Microchim. Acta. 134 (2000) 1–7.
[4] F.G. Bessoth, O.P. Naji, J.C.T. Eijkel, A. Manz, Towards an on-chip gas chromatograph: the development of a gas injector and a dc plasma emission detector, J. Anal. At. Spectrom. 17 (2002) 794–799.
[5] T. Cserfalvi, P. Mezei, P. Apai, Emission studies on a glow discharge in 1 atmospheric pressure air using water as a cathode, J. Phys. D 26 (1993) 2184–2188.
[6] P. Mezei, T. Cserfalvi, M. Janossy, Pressure dependence of the atmospheric electrolyte cathode glow discharge spectrum, J. Anal. At. Spectrom. 12 (1997) 1203–1208.
[7] P. Mezei, T. Cserfalvi, M. Janossy, Szöcs, H.J. Kim, Similarity laws for glow discharges with cathodes of metal and an electrolyte, J. Phys. D 31 (1998) 2818–2825.
[8] T. Cserfalvi, P. Mezei, Subnanogram sensitive multimetal detector with atmospheric electrolyte cathode glow discharge, J. Anal. At. Spectrom. 18 (2003) 596–602.
[9] H.J. Kim, J.H. Lee, M.Y. Kim, T. Cserfalvi, P. Mezei, Development of open-air type electrolyte-as-cathode glow discharge-atomic emission spectrometry for determination of trace metals in water, Spectrochim. Acta Part B 55 (2000) 823–831.
[10] W.C. Davis, R.K. Marcus, An atmospheric pressure glow discharge optical emission source for the direct sampling of liquid media, J. Anal. At. Spectrom. 16 (2001) 931–937.
[11] R.K. Marcus, W.C. Davis, An atmospheric pressure glow discharge optical emission source for the direct sampling of liquid media, Anal. Chem. 73 (2001) 2903–2910.
[12] W.C. Davis, R.K. Marcus, Role of powering geometries and sheath gas composition on operation characteristics and the optical emission in the liquid sampling-atmospheric pressure glow discharge, Spectrochim. Acta Part B 57 (2002) 1473–1486.
[13] M.R. Webb, F.J. Andrade, G. Gamez, R. McCrindle, G.M. Hieftje, Spectroscopic and electrical studies of a solution-cathode glow discharge, J. Anal. At. Spectrom. (2005) 1218–1225.
[14] Y. Yin, J. Messier, J.A. Hopwood, Miniaturization of inductively coupled plasma sources, IEEE Trans. Plasma. Sci. 27 (1999) 1516–1524.
[15] J.A. Hopwood, Microfabricated inductively coupled plasma generator, J. Microelectromech. Syst. 9 (2000) 309–313.
[16] F. Iza, J. Hopwood, Influence of operating frequency and coupling coefficient on the efficiency of microfabricated inductively coupled plasma sources, Plasma Sources Sci. Technol. 11 (2002) 229–235.
[17] D. Liang, M.W. Blades, Atmospheric-pressure capacitively coupled plasma spectral lamp and source for the direct analysis of conducting solid samples, Spectrochim. Acta Part B 44 (1989) 1049–1057.
[18] M.W. Blades, The response of the inductively-coupled argon plasma to solvent plasma load-spatially-resolved maps of electron-density obtained from the intensity of one argon line, Spectrochim. Acta Part B 49 (1994) 1231–1250.
[19] S.D. Anghel, T. Frentiu, E.A. Cordos, A. Simon, A. Popescu, Atmospheric pressure capacitively coupled plasma source for the direct analysis of non-conductive solid samples, J. Anal. At. Spectrom. 14 (1999) 541–545.
[20] S.Y. Lu, C.W. LeBlanc, M.W. Blades, Analyte ionization in the furnace atomization plasma excitation spectrometry source — spatial and temporal observations, J. Anal. At. Spectrom. 16 (2001) 256–262.
[21] A. Bass, C. Chevalier, M.W. Blades, A capacitively coupled microplasma (CC mu P) formed in a channel in a quartz wafer, J. Anal. At. Spectrom. 16 (2001) 919–921.
[22] H. Yoshiki, Y. Horiike, Jpn. J. Appl. Phys. 40 (2001) L360–L362.
[23] A.M. Bilgic, E. Voges, U. Engel, J.A.C. Broekaert, A low-power 2.45 GHz microwave induced helium plasma source at atmospheric pressure based on microstrip technology, J. Anal. At. Spectrom. 15 (2000) 579–580.
[24] A.M. Bilgic, U. Engel, E. Voges, M. Kückelheim, J.A.C. Broekaert, A new low-power microwave plasma source using microstrip technology for atomic emission spectrometry, Plasma Sources Sci. Technol. 9 (2000) 1–4.

[25] J. Hopwood, F. Iza, Ultrahigh frequency microplasmas from 1 pascal to 1 atmosphere, J. Anal. At. Spectrom. 19 (2004) 1145–1150.
[26] J. Franzke, K. Kunze, M. Miclea, K. Niemax, Microplasmas for analytical spectrometry, J. Anal. At. Spectrom. 18 (2003) 802–807.
[27] C. Penache, M. Miclea, A. Bräuning-Demian, O. Hohn, S. Schössler, T. Jahnke, K. Niemax, H. Schmidt-Böcking, Characterization of a high-pressure microdischarge using diode laser atomic absorption spectroscopy, Plasma Sources Sci. Technol. 11 (2002) 476–483.
[28] M. Miclea, K. Kunze, G. Musa, J. Franzke, K. Niemax, The dielectric barrier discharge — a powerful microchip plasma for diode laser spectrometry, Spectrochim. Acta Part B 56 (2001) 37–43.
[29] K. Kunze, M. Miclea, G. Musa, J. Franzke, C. Vadla, K. Niemax, Diode laser-aided diagnostics of a low-pressure dielectric barrier discharge applied in element-selective detection of molecular species, Spectrochim. Acta Part B 57 (2002) 137–146.
[30] M. Miclea, K. Kunze, J. Franzke, K. Niemax, Plasmas for lab-on-the-chip applications, Spectrochim. Acta Part B 57 (2002) 1585–1592.
[31] K. Kunze, M. Miclea, J. Franzke, K. Niemax, The dielectric barrier discharge as a detector for gas chromatography, Spectrochim. Acta Part B 58 (2003) 1435–1443.
[32] Z. Zhu, S. Zhang, J. Xue, X. Zhang, Application of atmospheric pressure dielectric barrier discharge plasma for the determination of Se, Sb and Sn with atomic absorption spectrometry, Spectrochim. Acta Part B 61 (2006) 916–921.
[33] R.J. Skelton Jr., H.-C.K. Chang, P.B. Farnsworth, K.E. Markides, M.L. Lee, Radio-frequency plasma detector for sulfur selective capillary gas-chromatographic analysis of fossil-fuels, Anal. Chem. 61 (1989) 2292–2298.
[34] J.A.C. Broekaert, The development of microplasmas for spectrochemical analysis, Anal. BioAnal. Chem. 374 (2002) 182–187.
[35] J. Franzke, K. Kunze, M. Miclea, K. Niemax, Microplasmas for analytical spectrometry, J. Anal. At. Spectrom. 18 (2003) 802–807.
[36] Karanassios, Microplasmas for chemical analysis: analytical tools or research toys? Spectrochim. Acta Part B 59 (2004) 909–928.
[37] J.A.C. Broekaert, V. Siemens, Some trends in the development of microplasmas for spectrochemical analysis, Anal. BioAnal. Chem. 380 (2004) 185–189.
[38] K.H. Becker, K.H. Schoenbach, J.G. Eden, Microplasmas and applications, J. Phys. D 39 (2006) R55–R70.
[39] J.R. Roth, Industrial plasma engineering, Principles, vol. 1, IOP Publishing, Philadelphia, 1995.
[40] U. Kogelschatz, B. Eliasson, W. Egli, From ozone generators to flat television screens: history and future potential of dielectric-barrier discharges, Pure Appl. Chem. 71 (1999) 1819–1828.
[41] A. Sobel, Plasma displays, IEEE Trans. Plasma. Sci. 19 (1991) 1032–1047.
[42] U. Kogelschatz, B. Eliasson, M. Hirth, Ozone generation from oxygen and air — discharge physics and reaction-mechanisms, Ozone: Sci. Eng. 10 (1988) 367–377.
[43] B. Eliasson, U. Kogelschatz, UV excimer radiation from dielectric-barrier discharges, Appl. Phys., B 46 (1988) 299–303.
[44] B.M. Penetrante, R.M. Brusasco, B.T. Merritt, G.E. Vogtlin, Pure Appl. Chem. 71 (1999) 1829–1835.
[45] B.M. Penetrante, M.C. Hsiao, J.N. Bardsley, B.T. Merritt, G.E. Vogtlin, A. Kuthi, C.P. Burkhart, J.R. Bayless, Plasma Sources Sci. Technol. 6 (1997) 251–259.
[46] G. Borcial, C.A. Anderson, N.M.D. Brown, Plasma Sources Sci. Technol. 12 (2003) 335–344.
[47] Z. Hubicka, M. Cad, M. Sicha, A. Churpita, P. Pokorný, L. Soukup, L. Jastrabik, Plasma Sources Sci. Technol. 11 (2002) 195–202.
[48] O. Goossens, E. Dekempeneer, D. Vangeneugden, R. Van de Leesta, Surf. Coat. Technol. 142–144 (2001) 474–481.
[49] R. Guchardi, P.C. Hauser, A capacitively coupled microplasma in a fused silica capillary, J. Anal. At. Spectrom. 18 (2003) 1056–1059.
[50] M. Laroussi, X. Lu, Room-temperature atmospheric pressure plasma plume for biomedical applications, Appl. Phys. Lett. 87 (2005) 113902.
[51] G.A. Eiceman, Z. Karpas, Ion Mobility Spectrometry, 2nd Ed.CRC Press, London, UK, 2005.
[52] W. Vautz, D. Zimmermann, M. Hartmann, J.I. Baumbach, J. Nolte, J. Jung, Ion mobility spectrometry for food quality and safety, Food Addit. Contam. 23 (11) (2006) 1064–1073.
[53] W. Vautz, J.I. Baumbach, J. Jung, Beer fermentation control using ion mobility spectrometry, J. Inst. Brew. 112 (2006) 157–164.
[54] M. Westhoff, P. Litterst, L. Freitag, B. Obertrifter, V. Ruzsanyi, J.I. Baumbach, Ion mobility spectrometry — a new method in the diagnostic approach to sarcoidosis?- Preliminary data, Eur. Respir. J. 28 (2006) 111S.
[55] J.I. Baumbach, M. Westhoff, Ion mobility spectrometry to detect lung cancer and airway infections, Spectrosc. Eur. 18 (2006) 22–27.
[56] S.J. Bos, S.M. van Leeuwen, U. Karst, From fundamentals to applications: recent developments in atmospheric pressure photoionization mass spectrometry, Anal. Bioanal. Chem. 384 (2006) 85–99.
[57] A. Raffaelli, A. Saba, Atmospheric pressure photoionization mass spectrometry, Mass Spectrom. Rev. 22 (5) (2003) 318–331.
[58] H. Borsdorf, H. Schelhorn, J. Flachowsky, H.R. Doring, J. Stach, Anal. Chim. Acta 403 (1–2) (2000) 235–242 JAN 3.
[59] G.A. Eiceman, Z. Karpas, Ion Mobility Spectrometry, 1st Ed.CRC Press, London, UK, 1994.
[60] R.G. Ewing, G.A. Eiceman, J.A. Stne, Proton-bound cluster ions in ion mobility spectrometry, Int. J. Mass Spectrom. 193 (1999) 57–58.
[61] E.D. Pellizzari, Electron capture detection in gas chromatography, J. Chromatogr. 98 (1974) 323–361.
[62] R.W.P. Pearse, A.G. Gaydon, The Identification of Molecular Spectra, Chapman and Hall LTD, London, 1950.
[63] P.L. Smith, C. Heise, J.R. Esmond, R.L. Kurucz, Atomic spectral line database from CD-Rom 23 of R.L. Kurucz, http://cfa-www.harvard.edu/amp/data/kur23/sekur.html.
[64] X.P. Lu, M. Laroussi, Dynamics of an atmospheric pressure plasma plume generated by submicrosecond voltage pulses, J. Appl. Phys. 100 (2006) 063302.
[65] A. Sublet, C. Ding, J.-L.- Dorier, C.h. Holenstein, P. Fayet, F. Coursimault, Atmospheric and sub-atmospheric dielectric barrier discharges in helium and nitrogen, Plasma Sources Sci. Technol. 15 (2006) 627–634.
[66] S.C. Brown, Basic Data in Plasma Physics, MIT Press, Cambridge, 1959.
[67] A. von Engel, Electric Plasmas: Their Nature and Uses, Taylor and Francis Ltd, London and New York, 1983.
[68] Hirschfelder, Curtis and Bird, Molecular Theory of Gases and Liquids, Wiley, New York, 1966.